

2013

# Monocyte depletion prior to intracerebral hemorrhage worsens cognitive and motor outcome

---

<https://hdl.handle.net/2144/12184>

*"Downloaded from OpenBU. Boston University's institutional repository."*

BOSTON UNIVERSITY  
SCHOOL OF MEDICINE

Thesis

**MONOCYTE DEPLETION PRIOR TO INTRACEREBRAL HEMORRHAGE  
WORSENS COGNITIVE AND MOTOR OUTCOME**

by

**NICHOLAS VETTE HUBBARD PETERS**

B.A., St. Olaf College, 2010

Submitted in partial fulfillment of the  
requirements for the degree of

Master of Arts

2013

Approved by

First Reader

---

Theresa A. Davies, Ph.D.  
Director, M.S. in Oral Health Sciences Program  
Adjunct Assistant Professor of Biochemistry

Second Reader

---

Michael Whalen, M.D.  
Associate Professor, Pediatric Critical Care Medicine  
Massachusetts General Hospital

## **ACKNOWLEDGEMENTS**

Thanks to Michael Whalen's lab for collaborating, mentoring, and teaching me, all in a friendly and supportive environment.

**MONOCYTE DEPLETION PRIOR TO INTRACEREBRAL HEMORRHAGE  
WORSENS COGNITIVE AND MOTOR OUTCOME**

**NICHOLAS VETTE HUBBARD PETERS**

Boston University School of Medicine, 2013

Major Professor: Theresa A. Davies, Ph.D., Director, M.S. in Oral Health Sciences Program and Adjunct Assistant Professor of Biochemistry

**ABSTRACT**

A number of studies have cited immune cell infiltration as a mechanism for secondary injury following intracerebral hemorrhage. However, the role of monocytes remains poorly understood. We hypothesized that monocytes are a beneficial cell type that help remove extravasated blood and other pathogenic substances that enter brain parenchymal tissue during a hemorrhagic stroke. Using macrophage Fas-induced apoptosis (MAFIA) mice, this study documents a time course of monocyte infiltration into brain tissue. We then systemically knocked down monocytes prior to initiating an intracerebral hemorrhage, and studied the motor and cognitive outcomes relative to a vehicle treated group.

The genetic alteration present in MAFIA mice causes the co-expression of green fluorescent protein and a suicide protein, exclusively in monocytes and dendritic cells. We established a time course of monocyte infiltration by counting cells expressing green fluorescent protein in brain parenchymal tissue at four time points after initiating a severe collagenase-induced hemorrhage. We found that at the 48-hour time point there was a

significant increase of immune cells infiltrating the core of the lesion relative to that observed at 6 hours and 24 hours, and non-significant decline at the 7-day time point.

Furthermore, the administration of AP20187 to MAFIA mice causes the dimerization of the suicide proteins, which initiates Fas-induced apoptosis selectively in cells expressing the suicide protein. By administering 10 $\mu$ L of AP20187 per animal for four consecutive days, we were able to knockdown monocytes both systemically and in brain parenchymal tissue following hemorrhage. To investigate the role of monocytes following intracerebral hemorrhage, we compared a monocyte-depleted group of MAFIA mice to a vehicle-treated group. Both groups underwent a collagenase-induced hemorrhage, and then were subjected to wire grip testing and Morris Water Maze. The group of monocyte-depleted MAFIA mice performed worse in wire grip testing ( $p < 0.02$ ), as well as in the Morris Water Maze test ( $p < 0.01$ ). Through the course of the 3-week experiment there was 50% mortality in the monocyte-depleted group, while no animals died in the vehicle treated group.

Both of the functional studies and the mortality data suggest that monocytes play an important role following intracerebral hemorrhage. The infiltration data suggests that monocytes are recruited to parenchymal tissue after 6 and 24 hours following hemorrhage and remain present for at least one week. This time frame offers a large window for therapeutic modulation of monocyte recruitment and/or function. Future studies should focus on identifying monocytes' mechanisms of action, as well as improving the MAFIA mouse model by controlling for the weight loss and the cause of profound splenomegaly observed in the monocyte-depleted group.

## TABLE OF CONTENTS

|  |      |
|--|------|
| Title  | i    |
| Reader's Approval Page                                   | ii   |
| Acknowledgements   | iii  |
| Abstract   | iv   |
| Table of Contents  | vi   |
| List of Tables   | viii |
| List of Figures  | ix   |
| List of Abbreviations                                    | x    |
| Introduction   | 1    |
| Methods  | 14   |
| Animals  | 14   |
| Knockdown of GFP Positive Cells                          | 15   |
| Collagenase Induced Intracerebral Hemorrhage             | 16   |
| Tissue Preparation and Florescent Microscopy             | 17   |
| Leukocyte Analysis via Flow Cytometry                    | 18   |
| Functional Behavior Testing                              | 18   |
| Results  | 21   |
| Intracerebral Hemorrhage Model and Monocyte Infiltration | 21   |
| Knockdown of GFP Positive Cell Infiltration              | 24   |
| Wire Grip Motor Test                                     | 27   |

|                               |    |
|-------------------------------|----|
| Morris Water Maze Test        | 28 |
| Anatomical Abnormalities      | 30 |
| Discussion                    | 31 |
| List of Journal Abbreviations | 38 |
| References                    | 39 |
| Vita                          | 43 |

## LIST OF TABLES

| Table | Title   | Page |
|-------|---|------|
| 1     | Potential Therapeutics to Ameliorate Secondary ICH Damage | 11   |
| 2     | Wire Grip Grading Rubric                                  | 19   |

## LIST OF FIGURES

| Figure | Title  | Page |
|--------|--|------|
| 1      | Organization of injurious mechanisms resulting from ICH  | 3    |
| 2      | Thrombin-induced secondary ICH injury                    | 7    |
| 3      | MAFIA Mouse Transgene Schematic                          | 14   |
| 4      | Experimental Timeline Schematic                          | 16   |
| 5      | Monocyte Infiltration Time Course                        | 22   |
| 6      | GFP Positive Cells Counts of Inflammation Time Course    | 23   |
| 7      | Peripheral Blood Flow Cytometry Analysis                 | 25   |
| 8      | Reduction of GFP Positive Cells in Brain Tissue          | 26   |
| 9      | Weight Loss Trend  | 27   |
| 10     | Wire Grip Data   | 28   |
| 11     | Morris Water Maze Data                                   | 29   |
| 12     | Spleen Comparison  | 30   |
| 13     | Varied Morphologies of GFP Positive Cell in Brain Tissue | 33   |
| 14     | Mortality Analysis                                       | 36   |

## ABBREVIATIONS

|                |  |
|----------------|--|
| BBB            | Blood-Brain Barrier  |
| CDC            | Center for Disease Control                                   |
| CSF-1          | Colony Stimulating Factor-1                                  |
| GFP            | Green Florescent Protein                                     |
| ICH            | Intracerebral Hemorrhage                                     |
| IL-1 $\beta$   | Interleukin 1 $\beta$ eta                                    |
| IRES           | Internal Ribosomal Entry Site                                |
| LNGFR          | Low-affinity Nerve Growth Factor Receptor                    |
| MAC            | Membrane Attack Complex                                      |
| MAFIA          | Macrophage Fas-Induced Apoptosis                             |
| MAPK           | Mitogen-Activated Protein Kinase                             |
| MMPs           | Matrix Metalloproteinases                                    |
| NF- $\kappa$ B | Nuclear Factor Kappa B                                       |
| PAR            | Protease Activated Receptor                                  |
| PBS            | Phosphate Buffered Saline                                    |
| PFA            | Paraformaldehyde   |
| RBC            | Red Blood Cell   |
| ROI            | Reactive Oxygen Intermediate                                 |
| TBI            | Traumatic Brain Injury                                       |
| TNF $\alpha$   | Tumor Necrosis Factor Alpha                                  |
| TUNEL          | Terminal Deoxynucleotidyl Transferase dUTP Nick End Labeling |

## INTRODUCTION

### *Stroke*

According to the Center for Disease Control (CDC), stroke is currently the fourth leading cause of death in the United States, behind only cardiovascular disease, cancer, and lower respiratory infections<sup>1</sup>. There are two primary types of stroke: ischemic stroke and hemorrhagic stroke. Ischemic strokes constitute about 85% of all strokes<sup>1</sup>, and occur when brain tissue does not receive sufficient blood flow due to blockage of vasculature. Hemorrhagic strokes are further classified by location, leading to two major subtypes: subarachnoid or intracerebral hemorrhages. Subarachnoid hemorrhages occur in the subarachnoid space, while intracerebral hemorrhages occur in brain parenchymal tissue<sup>2</sup>.

### *Intracerebral Hemorrhage*

Intracerebral hemorrhage (ICH) is the presence of extravasated blood in brain parenchymal tissue, originating from a ruptured blood vessel<sup>2,3</sup>. It is the second most common form of stroke, and yet there is no pharmaceutical treatment to date<sup>4</sup>. The leading cause of spontaneous ICH is the rupturing of microaneurysms at the junction of blood vessels<sup>5</sup>. Often times these microaneurysms are induced by chronic hypertension in brain vasculature<sup>5</sup>. Other causes of ICH include: amyloid angiopathy, tumors, arteriovenous malformations and fistulas, and cavernous angiomas<sup>6</sup>. There is significant morbidity and mortality associated with ICH<sup>7,8,9</sup>. In fact, the Oxfordshire Community Stroke Project found the actuarial risk of death in persons whom had experience a primary intracerebral

hemorrhage to be 62% within a year of hemorrhage<sup>7</sup>.

Other studies, have found a correlation between worse outcomes and the advancing age of incident<sup>6,10,11</sup>. A prospective study of 166 patients who experienced ICH, conducted by Daverat et al., found that age was the factor most strongly correlated to survival at 6 months post ICH<sup>10</sup>. Furthermore, Gong et al. reported greater neurological impairment and more severe edema in older cohorts of a rodent study<sup>11</sup>.

### ***Pathological Mechanisms of Intracerebral Hemorrhage***

**Primary and Secondary Injury:** Intracerebral hemorrhage is a complex and multifaceted injury (Figure 1). It can be lethal shortly after ictus, or possibly even weeks afterward due to continued pathophysiological mechanisms that have been reported to persist at least 4 weeks<sup>12</sup>. To help evaluate and analyze the pathological mechanisms of ICH two categories have been established: primary and secondary injury mechanisms<sup>13</sup>.

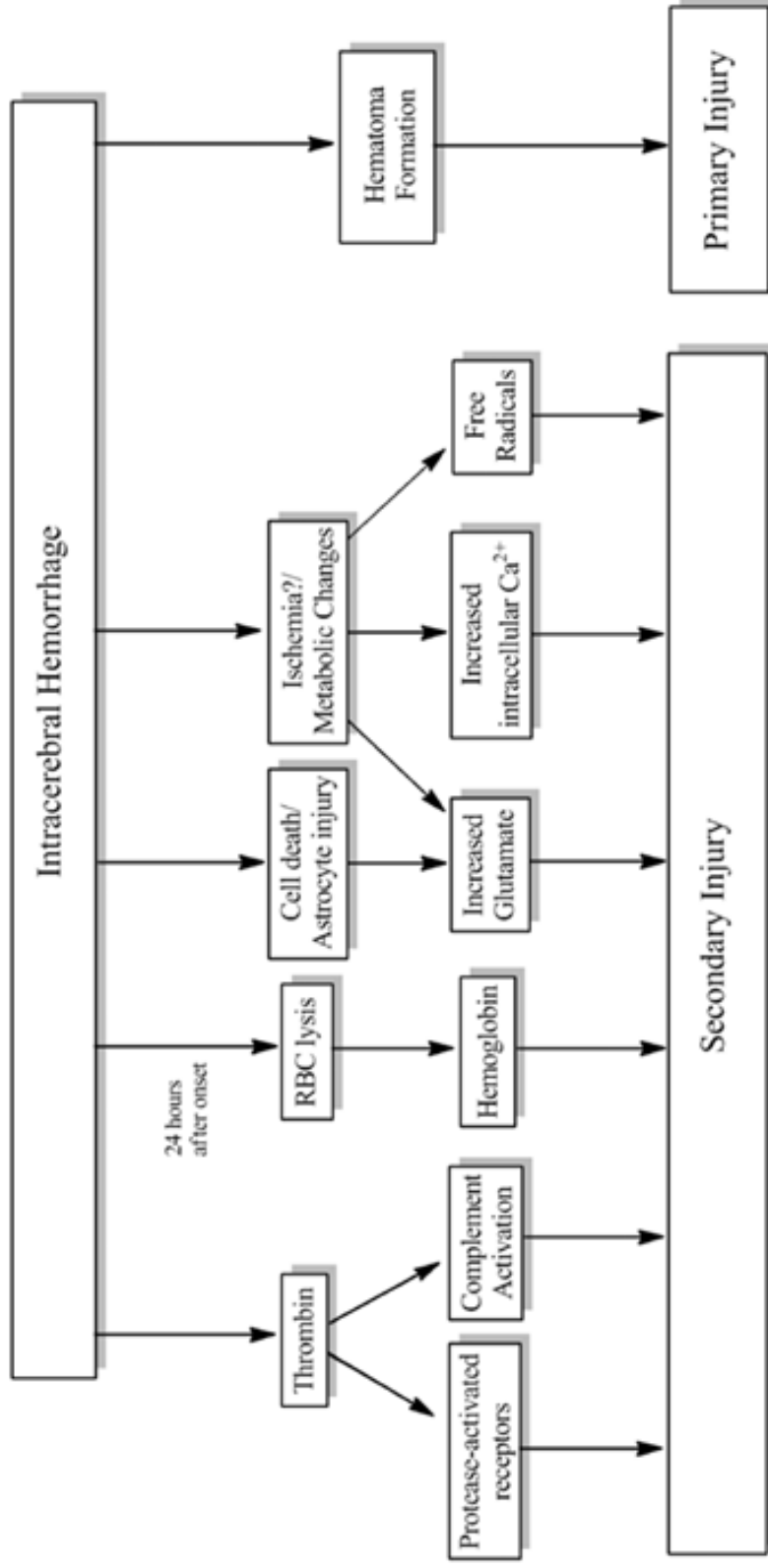


**Figure 1. Organization of injurious mechanisms resulting from ICH.** Primary injury follows directly from hematoma formation. It is characterized by mechanical disruption and increased pressure, and presents clinically as elevated intracranial pressure, midline shift, and functional deficits. Secondary injury results from the very complex interplay between the downstream effects of thrombin, extravasated RBCs, complement activation, inflammation, and, possibly, ischemia. (Figure taken and adapted from Babu et al., 2012.)

### ***Primary Injury Mechanisms***

**Hematoma Formation and Mass Effect:** The majority of brain injury stemming from ICH typically occurs within the first few hours<sup>13</sup> and is a direct result of hematoma formation and of mass effect<sup>3,13</sup>. While the majority of hemorrhages stop bleeding shortly after incident<sup>2</sup>, a number of studies have noted a significant percentage of cases in which hematomas continue to enlarge after 20 hours<sup>14,15,16</sup>. Continued hematoma enlargement hours after onset, and hematomas that have secondary bleeds have deleterious effects on patient outcomes, by increasing mass effect<sup>5</sup>. Hemorrhage growth and edema have a synergistic relationship, and together raise intracranial pressure, leading to further mass effect damage<sup>10</sup>. Unfortunately, an optimal therapy that combats primary ICH injury has not yet been identified<sup>13</sup>. However, even after patients stabilize, many continue to deteriorate without evidence of hemorrhage growth<sup>17</sup>, which suggests the potential for clinical intervention to ameliorate secondary mechanisms of damage.

### ***Secondary Injury Mechanisms***

**Thrombin:** Thrombin is a protein normally present in the blood in its inactive form – prothrombin. However, during ICH both the intrinsic and extrinsic coagulation cascades are activated, which cleave prothrombin to its active form: thrombin<sup>18</sup>. The effect of thrombin in the presence of brain parenchymal tissue has been studied extensively<sup>19,20,21,22</sup>. It has been reported that at low concentrations (under 100 nanomolar) thrombin is neuroprotective<sup>21</sup> but at high concentrations (above 500 nanomolar) thrombin causes damage<sup>22</sup>. Also, Xi *et al.* reported that upon clotting, 1 mL of whole blood can

produce 1-2 nanomoles of thrombin<sup>18</sup>. Thus, in the scenario of intracerebral hemorrhage the blood alone that enters parenchymal tissue produces potentially pathological amounts of thrombin. It has also been shown that brain tissue itself produces prothrombin<sup>4</sup>, which upon activation by either internal or external coagulation cascade further exacerbates local thrombin levels in brain tissue. Studies have also shown that thrombin is continuously released from cerebral hematomas for 14 days after the initial clot formation<sup>23</sup>, suggesting thrombin-induced secondary injury plays a role in patient deterioration well after the onset of ICH.

Together these factors culminate in a high, and sustained, concentration of thrombin in brain parenchymal tissue following intracerebral hemorrhage. Thrombin-induced injury is complex (Figure 2). It can cause damage via the activation of complement, and to parenchymal tissues through the activation of protease activated receptors (PARs) and the RhoA receptor.

Thrombin activation of the complement system occurs primarily by cleavage of C3 into C3a anaphylatoxin and C3b in conjunction with C4b2a<sup>24</sup>. C4b2a enzymatically cleaves C5, and then C5b is able to assemble the membrane attack complex (MAC) on plasma membranes<sup>24</sup>. Complement induced cell death may be responsible for neuronal and endothelial cell death, as well as the lysis of infiltrating RBCs<sup>25</sup>. Endothelial cell death is important as it could exacerbate bleeding and/or increase blood-brain barrier (BBB) breakdown following ICH. Complement induced lysis of RBCs introduces hemoglobin into the extracellular space, which exerts oxidative stress on the surrounding tissues<sup>13</sup>.

The second effect of thrombin is through its activation of protease-induced

receptors (PAR). Thrombin can activate PARs 1, 3, and 4<sup>26</sup>, as well as RhoA<sup>13,18</sup>, which is also within the PAR superfamily. Although the mechanism is unknown, thrombin activation of RhoA induces apoptosis in neurons and astrocytes<sup>27</sup>, and RhoA inhibitors have been shown to mitigate thrombin-mediated cell death<sup>18</sup>. Thrombin activation of PARs 1, 3, and 4 have been shown to up-regulate the phosphorylation of mitogen-activated protein kinases (MAPK)<sup>13,28,29</sup>. Neuronal MAPKs recruit microglia, and increase neuronal damage measured by terminal deoxynucleotidyl transferase dUTP nick end labeling (TUNEL) staining<sup>29</sup>. Recruitment and subsequent activation of microglia to the area surrounding the injury leads to an increase in inflammatory cytokines, specially tumor necrosis factor alpha (TNF  $\alpha$ ) and interleukin-1 beta (IL-1 $\beta$ )<sup>30</sup>. Secondary to the increase of TNF  $\alpha$  and IL-1 $\beta$ , Nuclear Factor  $\kappa$ B (NF- $\kappa$ B) is activated<sup>31</sup>, resulting in cell death via DNA fragmentation<sup>32</sup>.

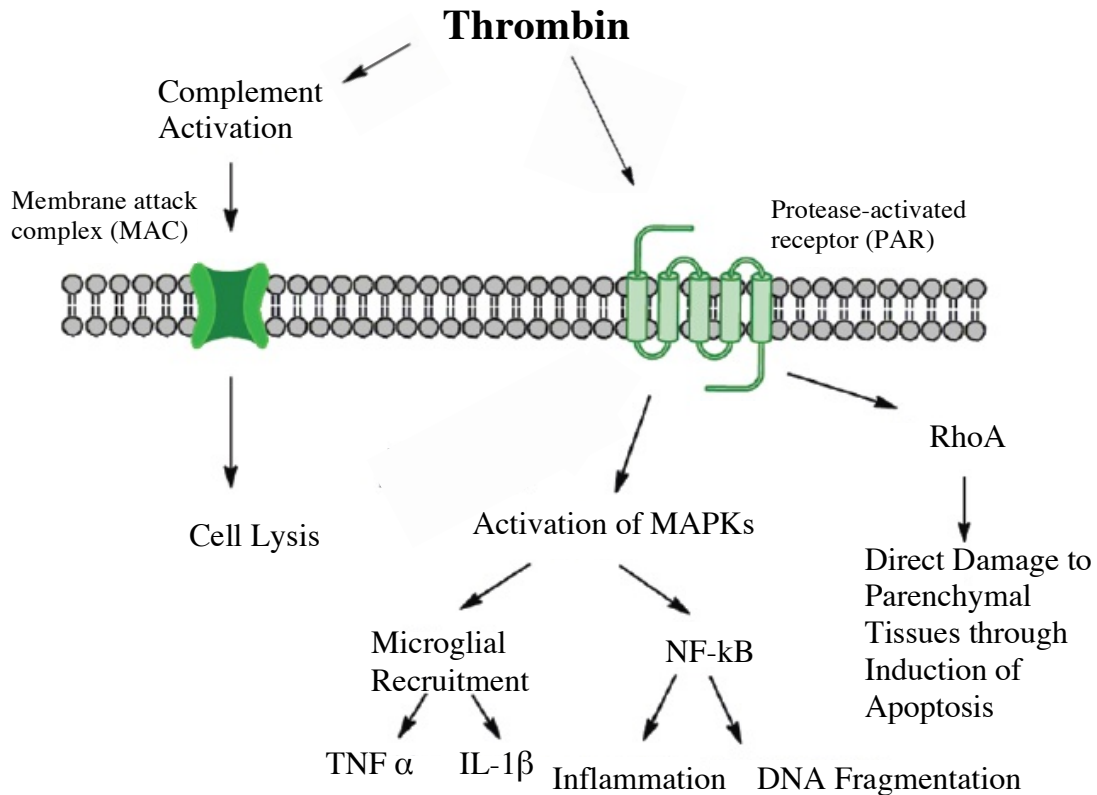


**Figure 2. Thrombin Induced Secondary ICH Injury.** Thrombin activates the complement system, which then is able to form the MAC and cause cell lysis. Alternatively, thrombin can trigger PARs causing a range of deleterious consequences. (Figure taken and adapted from Babu et al., 2012).

**Edema:** Previous studies have illustrated the correlation between brain edema and poor clinical outcomes<sup>5,33</sup>. Edema is a dynamic process, driven by diverse factors at different time points following ICH. Acute phase (within hours of ICH) edema is dictated by hydrostatic pressure as serum from extravasated blood diffuses into the tissues surrounding the hemorrhage<sup>5</sup>, subacute phase (>2 days post ICH) edema is characterized by a more porous BBB brought on by thrombin-induced endothelial cell death<sup>5,13</sup>, and late

phase edema is driven by RBC lysis, and ensuing oxidative stress from local hemoglobin<sup>5</sup>.

**Inflammatory Response:** The inflammatory response to ICH consists of both cellular and molecular constituents. The cellular component includes resident microglia and peripheral leukocytes that infiltrate parenchymal tissue<sup>34</sup>. The molecular elements of the inflammatory response are produced by the cellular component, and consist of cytokines, chemokines, proteases, and reactive oxygen intermediates (ROI)<sup>34,35</sup>.

The first cells that display inflammatory behavior are the resident microglia<sup>34</sup>. While the primary goal of microglia is hypothesized to clear the hematoma, they also release a variety of cytokines and ROIs<sup>36-39</sup>. Among the cytokines known to be produced by activated microglia are TNF  $\alpha$  and IL-1 $\beta$ <sup>13,34</sup>, which both induce peripheral leukocytes to infiltrate brain parenchymal tissue, as well as exacerbate cerebral edema. While early microglial activity may be deleterious, they continue to be activated for 3-4 weeks after ictus, and thus require further investigation to best understand how to modulate their activity following ICH<sup>34</sup>.

Research in both animal and clinical studies have offered evidence of leukocytes playing a role in ICH<sup>12,40-44</sup>. In a mouse collagenase-induced hemorrhage model, Wang and Tsirka reported that neutrophil infiltration began as early as 4 hours, and peaked at 3 days<sup>41</sup>. Neutrophils and monocytes are known to release inflammatory cytokines and ROIs (similar to microglia), as well as pro-inflammatory proteases, specifically matrix metalloproteinases (MMPs)<sup>39,45</sup>. MMPs disrupt the BBB by degrading intracellular matrix, which facilitates further leukocyte infiltration<sup>13</sup>. In a study published by Wang and Tsirka in 2005, inhibition of MMPs concurrently provided neuroprotection and a reduction in

neutrophil infiltration in a rodent model<sup>38</sup>. The exact role and mechanisms of neutrophil action following ICH is the subject of continued investigation.

Monocytes are another type of leukocyte known to infiltrate brain tissue following injury, and have been implicated in neuronal cell death and functional deficit<sup>46,47</sup>. In addition to entrance during a hemorrhage, monocytes are drawn to the site of injury by chemokines, primarily CCL2<sup>48</sup>. CCL2 is synthesized at a basal level by epithelial cells, but its production is increased by 290 fold in response to elevated IL-1 $\beta$  and TNF  $\alpha$  as seen following ICH<sup>46</sup>. However, besides in response to the massive up-regulation of CCL2, little is known about how monocytes enter brain parenchymal tissue and their role once present at the site of injury<sup>46</sup>.

Monocytes' ability phagocytosis RBCs and other dead and dying cells suggests they may play a critical role in the clean up process. However, their ability to synthesize pro-inflammatory cytokines, such as IL-1 $\beta$  and TNF  $\alpha$ , encourage further immune cell infiltration through disruption of the BBB by the secretion of MMPs, and ability to generate ROIs, suggests their potential to be major contributors of secondary injury following ICH.

### ***Potential of Research in Stroke***

According to the US Department of Health and Human Services, stroke has been among the top four leading causes of death for over five decades in the United States<sup>49</sup>. It also is a growing problem as hospitalizations for ICH increased by 18-19% from 1990 to 2000<sup>3,50</sup>. These statistics along with the country's aging population, suggests that stroke is

poised to continue being a leading health concern in the foreseeable future<sup>51</sup>. It is therefore an important avenue of study, and one with tremendous potential to increase overall health and welfare within our nation, as well as across the globe. The current study focuses on the stroke subtype, intracerebral hemorrhage, and attempts to further elucidate the pathological mechanisms leading to poor outcomes with the hope that therapeutic strategies can be realized from a better understanding of the nature of ICH.

Primary injury from ICH occurs rapidly following ictus, which limits therapeutic options as most strokes occur outside of a hospital setting. Surgical management, such as clot resection and hemorrhage evacuation to reduce intracranial pressure, has not shown consistent benefit<sup>13,52</sup>. Other approaches have shown promise, but also carry the risk of serious complications: treatment with recombinant factor VIIa first appeared promising, but in phase III clinical trial thromboembolic complications were problematic<sup>5,53,54</sup>. Unfortunately, an optimal therapy for the primary injury of ICH has not yet been determined<sup>13</sup>.

The interconnected nature of the pathophysiological mechanisms of secondary ICH injury complicates therapeutic strategies. With recent advances into the understanding of the pathological mechanisms of ICH, therapies to ameliorate secondary damage of ICH are currently being investigated<sup>13,17,34</sup>, and are summarized below in (Table 1). This study aims to further characterize the role of monocytes in secondary ICH damage, with the hope that modulation of monocyte activity will be a potential therapeutic for patients suffering from ICH in the future.

**Table 1. Potential Therapeutics to Ameliorate Secondary ICH Damage.**

\*The clinical study of NXY-059 is currently ongoing. \*\*Kane et al did not report on systemic depletion of a specific leukocyte types, but rather systemic depletion of all leukocytes via sub-lethal radiation. (Table taken and adapted from Wang and Doré, 2007).

| <i>Target</i>   | <i>Strain</i>          | <i>Reference</i>  |
|---|------------------------|---|
| <i>Leukocyte Infiltration</i><br>Global immunosuppression through irradiation**   | Rat                    | Kane et al (1992)   |
| <i>Microglial Activation</i><br>Microglial/macrophage inhibitory factor (MIF)<br>Minocycline  | Mouse<br>Rat           | Wang et al (2003) & Wang and Tsirka (2005)<br>Power et al (2003)        |
| <i>Cytokines</i><br>TNF $\alpha$ -specific antisense oligodeoxynucleotide<br>Adenosine A <sub>2A</sub> receptor agonist<br>Overexpression of IL-1ra | Rat<br>Rat<br>Rat      | Mayne et al (2001a)<br>Mayne et al (2001b)<br>Masada et al (2001, 2003) |
| <i>Matrix Metalloproteinases (MMPs)</i><br>BB-1101<br>GM6001  | Rat<br>Mouse           | Rosenberg & Navratil (1997)<br>Wang and Tsirka (2005)                   |
| <i>Reactive Oxygen Species</i><br>$\alpha$ -Phenyl- <i>N</i> - <i>tert</i> -butyl nitron<br>NXY-059<br>NXY-059                                      | Rat<br>Rat<br>Clinical | Aronowski & Hall (2005)<br>Peeling et al (2001)<br>Green and Ashwood *  |
| <i>Heme Oxygenases</i><br>Tin-mesoporphyrin IX<br>Tin-protoporphyrin<br>Zinc protoporphyrin   | Pig<br>Rat<br>Rat      | Wagner et al (2000)<br>Huang et al (2002)<br>Gong et al (2006)          |
| <i>Ferric Iron</i><br>Deferoxamine  | Rat                    | Wan et al (2006)  |

### ***Specific Area of Study***

Brain inflammation causes secondary damage and can drastically affect the survivability and outcome of patients who suffer an ICH<sup>7</sup>. Research to date has primarily investigated the role of microglial activation, neutrophil infiltration, cytokine levels, MMPs, and ROIs. However, the role of monocytes following ICH remains largely unexplored. The methods of entry into brain tissue, the circumstantial expression of cell surface markers, the time course of monocyte infiltration, the production of cytokines, phagocytic behavior, and synergistic effects with other cell types are all areas in need of study. Research in these areas will better allow potential therapeutic strategies to modulate the presence and/or effects of monocytes following ICH.

### ***Specific Study Aims/Objectives***

As shown in previous studies, a robust immune response, both systemic and local, occurs following a stroke. The profile of the immune cells infiltrating brain parenchymal tissue has been investigated, however the functions and specific role of these cells, in particular monocytes, remains unclear.

The goal of this study is to further understand the role of monocytes in brain parenchymal tissue following a hemorrhagic stroke. In the study, we will specifically investigate:

- (1) Quantitative assessment of monocytes in the core and peripheral regions of the hemorrhage. This knowledge will both demonstrate inflammatory cell infiltration and document its time course following hemorrhage.

- (2) Then, using the transgenic MAFIA mice, we will knockdown the animal's monocytes from before hemorrhage to the peak of inflammatory cell infiltration following hemorrhage, determined in aim one.
- (3) Cognitive and motor testing will be performed in dimerizer and vehicle groups to determine the effects of depleting monocytes on cognitive and motor functioning, in a hemorrhagic stroke model.

Using the Macrophage Fas-Induced Apoptosis (MAFIA) mice, macrophages were readily identifiable because green fluorescent protein (GFP) is encoded into colony stimulating factor-1, found primarily in macrophages and dendritic cells. These cells are can also be selectively depleted through Fas-activated apoptosis. We hope that increased knowledge of the function and effects of monocytes can advance the clinical treatment of patients who have suffered a stroke.

## MATERIALS AND METHODS

### *Animals*

Macrophage Fas-Induced Apoptosis (MAFIA) mice were procured from Jackson Laboratories and were housed in a climate controlled ( $23\pm 1^{\circ}\text{C}$ ) and ventilated environment, with *ad libitum* access to food and water. Mice between 4 and 20 weeks of age were used for experiments. All housing, transportation, and procedures were in compliance with Institutional Animal Care and Use Committee of Massachusetts General Hospital.

MAFIA mice have been manipulated to co-express green fluorescent protein (GFP) and a suicide protein, on cells synthesizing Colony Stimulating Factor-1 (CSF-1). The genetic alteration was introduced onto the CSF-1 receptor, which is specific to monocytes and dendritic cells. A schematic is represented (Figure 3) below to show the transgene. The suicide gene consists of: an internal ribosome entry site (IRES) to initiate synthesis, a modified low-affinity nerve growth factor receptor (LNGFR) directly bound to two human FKBP subunits to facilitate binding to neighboring suicide proteins, and human Fas to initiate apoptosis when activated<sup>55</sup>.



**Figure 3. MAFIA Mouse Transgene Schematic.** Synthesis of this gene allows for the co-localization of green fluorescent protein and the suicide motif on monocytes and dendritic cells. (Figure taken from Burnett et al., 2004).

### ***Knockdown of GFP Positive Cells***

AP20187 (Clontech Laboratories, Mountain View, CA, USA) is the dimerizing agent that causes two FKBP portions of neighboring suicide proteins to dimerize, which causes the activation of the Fas domain of the suicide gene, leading to apoptosis. AP20187 was dissolved in pure ethanol to form a 1mM stock solution, which was then diluted 1:2500 with a mixture of 4% ethanol, 10% PEG-400, 1.7% Tween, and 84.3% water. The vehicle solution was solely the ethanol, PEG-400, Tween, and water in the concentrations mentioned above.

Mice were administered either the dimerizer or the vehicle treatment for 4 consecutive days. The knockdown group received 10 $\mu$ L of the dimerizer mixed into 290 $\mu$ L of the vehicle solution, while the vehicle treated group received 300 $\mu$ L of pure vehicle solution. Under light anesthesia of 2% isoflurane, the mice were given intravenous injections the first day and intraperitoneal injections the remaining 3 days of treatment. Figure 4 is a timeline schematic that illustrates the relative time points of treatment, injury, and motor testing.

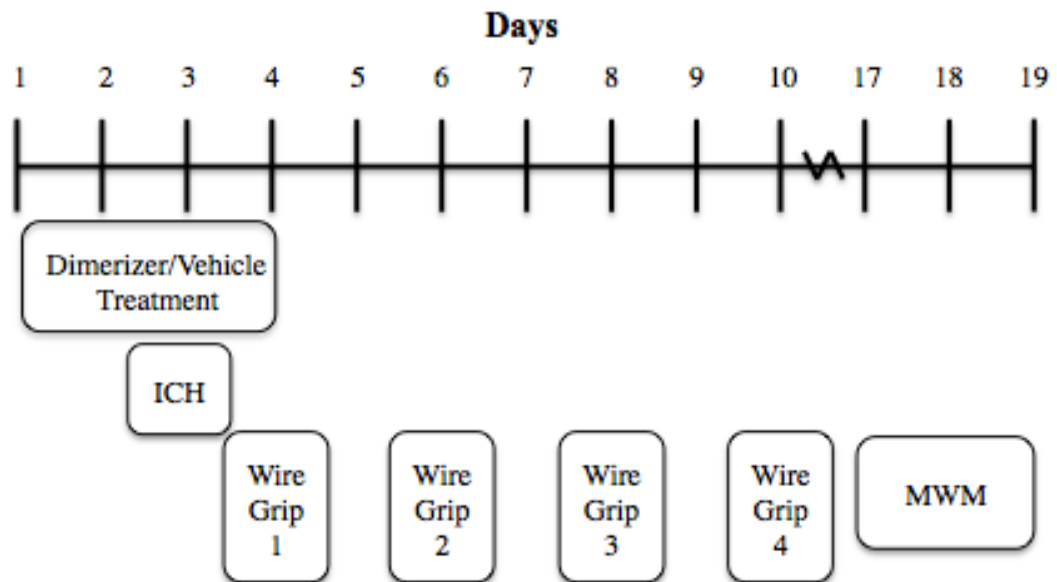


**Figure 4. Experimental Timeline Schematic.**

### ***Collagenase Induced Intracerebral Hemorrhage***

The mice underwent the intracerebral hemorrhage surgery on the third day of dimerizer/vehicle treatment. The mice were placed in a chamber and exposed to 65% nitrogen, 33% oxygen, and 2% isoflurane. Once anesthetized and unresponsive to a pressure stimulus, the mice were then secured in a stereotactic frame by a nose cone and bilateral ear bars. The nose cone continued to deliver the anesthetic gas mixture through the duration of the surgical procedure.

A small scalp incision was made to expose the animal's skull, and a 1mm diameter craniotomy was performed at the stereotactic coordinates of 1mm anterior to bregma, and 2mm lateral of the sagittal suture. A 32-gauge needle was inserted through the craniotomy to a depth between 3mm and 3.5mm, allowing the bore of the needle to open into the striatum. Over 2.5 minutes, 0.5  $\mu$ L of Type IV collagenase (0.03 U/0.04  $\mu$ L) was injected

into brain parenchymal tissue. The needle was then left in place for another 3.5 minutes to ensure that the collagenase diffused into the appropriate brain region. Once the needle was retracted, the skin incision was closed with interrupted sutures and the mice were allowed to recover at room temperature.

### ***Tissue Preparation and Florescent Microscopy***

Mice were placed in a chamber and deeply anesthetized by exposure to 63% nitrogen, 32% oxygen, and 5% isoflurane. They were then given an intraperitoneal injection between 250 and 350  $\mu$ L of Avertin (tribromoethanol, 20mg/mL). Once mice were unresponsive to a minor pain stimulus, their thoracic cavity was opened and a small incision was made in the right atrium of the heart. Then a syringe was positioned in the left ventricle and the animal was perfused with 15-20mL of 4% paraformaldehyde (PFA). The brain was then retrieved, and placed overnight in 4% PFA at room temperature. The brain was then dehydrated in 30% sucrose for 1-3 days.

The brain was then frozen in a bath of isopentane alcohol with dry ice. Then using a Microm HM525 (ThermoFisher Scientific Inc., Massachusetts, USA) the brain was sliced in the coronal plane, in 14 micron sections. Slides were prepared with a representative slice of tissue every 200-250 microns through the length of the lesion. Using a Nikon Eclipse Ti-S florescent microscope (Nikon, Tokyo, Japan) and NIS-Elements BR300 SP7 software, we captured images and counted fluorescently labeled GFP cells in x200 fields, selected from 6 – 8 tissue sections. Each animal had 16 fields counted through the length of the lesion, 8 core fields and 8 peripheral fields.

### ***Leukocyte Analysis via Flow Cytometry***

First, mice were heavily anesthetized with a 5% isoflurane as described above in the tissue preparation section. A heparin-coated syringe was then inserted into the thoracic cavity, and blood was drawn transcardially. The sample is separated by centrifugation at 450g and at 20°C. After removing the plasma, ACK Lysing Buffer (Lonza, Basel, Switzerland) was then added, at a ratio of 5:1 and gently mixed for 30 minutes. The sample was again centrifuged with the settings stated above, and the remaining cells were pelleted. The lysed red blood cells and lysing buffer were then removed.

The nuclear dye, Red Dot (Biotium, Hayward, CA, USA), was then added to the samples to facilitate analysis. Samples were incubated with the Red Dot dye for 15 minutes and after a final wash in PBS, the samples were loaded into a BD Accuri C6 Flow Cytometer (San Jose, CA, USA) for analysis.

### ***Functional Behavior Testing***

**Wire Grip:** Mice were administered the wire grip test on days 4, 6, 8, and 10, as illustrated above in Figure 4. The testing apparatus consisted of two wooden dowels, each measuring 1.5cm in diameter, suspended a wire 50cm above a bench top. The wire measured 2mm in diameter and was held taut between the two dowels. The test included 3 consecutive trials, in which mice were placed in the center of the wire. Each trial lasted 60 seconds, after which time removed from the wire and the trial would be scored 0-5

according to the grading rubric below in Table 1. The lowest score that describes the behavior exhibited by the mouse during a trial was the score assigned.

**Table 2. Wire Grip Grading Rubric.**

|   |  |
|---|--|
| 0 | A mouse falls while trying to traverse the wire, or while trying to climb down a dowel.  |
| 1 | A mouse stays on the apparatus for the entire 60 seconds, but while traversing the wire the mouse exhibits sided-weakness and/or uncoordinated movements, indicative of hemiparesis.     |
| 2 | A mouse stays on the apparatus for the entire 60 seconds, but the mouse does not wrap its tail around the wire and/or dowel.   |
| 3 | A mouse stays on the apparatus for the entire 60 seconds, and demonstrates tail wrapping. However, the mouse does not progress from the wire to one of the dowels.                       |
| 4 | A mouse stays on the apparatus for the entire 60 seconds, demonstrates tail wrapping, and mounts a dowel, but does not attempt, or finish, climbing down the dowel toward the bench top. |
| 5 | The mouse successfully traverses the wire without any indication of hemiparesis, demonstrates tail wrapping, and climbs down the dowel onto the bench top in under 60 seconds.           |

**Morris Water Maze:** The complete test included five hidden trials and a probe trial, spread over two days, followed by two visible trials and final probe trial on the third day. Mice were allowed to dry off and rest for at least 20 minutes between trials. Water maze testing was started on day 17, two weeks after the animals received a hemorrhage.

An opaque, white, plastic, 1meter diameter tank was filled with room temperature water. Four distinct symbols (a circle, triangle, square, and star) were placed on the inside of the tub equidistantly spaced, and just above the water line. A clear, plastic, circular platform, with a 10cm diameter, was positioned 15cm from the edge of the tank between the circle and square symbols. The water level was adjusted so that the surface of the

platform was 1 centimeter below water level during hidden trials, and 1 cm above water level during visible trials. Also during visible trials, a strip of red tape was placed around the exposed parameter of the platform, allowing the mice to see the platform from water level.

For hidden trials the tank was set to the above specifications, with the platform submerged. Mice were then placed in the water, directly in front of one of the symbols and allowed to swim freely for 90 seconds or until they climbed onto the platform. If by 90 seconds they had not yet found the platform, they were placed on the platform and allowed a few seconds to become acquainted with their position within the tank. An animal's score for a single hidden trial score was calculated as the average of four separate swims, each swim starting from a different symbol. Visible trials are conducted similarly, however the water level was lowered to make the platform visible to the mice.

In probe trials the platform was removed from the tank. Mice were placed into the water between the star and triangle symbols near the tank's edge, opposite to the location where the platform had been. Mice were allowed to swim freely for 1 minute, before being rescued from the water.

A digital camera placed above the tank recorded the mouse's movement during probe trials. Version 4.80 of ANY-Maze software (Stoelting Co, Wood Dale IL, USA) calculated the time the mouse spent in the quadrant where the platform had been during the hidden and visible trials.

## RESULTS

### *Intracerebral Hemorrhage Model and Monocyte Infiltration*

Deposition of collagenase into the animal's striatum caused an ipsilateral intracerebral hemorrhage with substantial hematoma formation, but with no detectable damage in the contralateral hemisphere. Using MAFIA mice, we hemorrhaged and sacrificed mice at 4 different time points to establish the infiltration time course. The time points we chose to study were 6 hours, 24 hours, 48 hours, and 7 days post ICH. To quantify monocyte infiltration, we perfused the mice at the given time points and prepared the tissue for florescent microscopy as described above. We counted GFP positive cells in 6 animals per time point, and each animal had 16 fields (8 core and 8 periphery). Figure 6 shows representative core fields at each time point.

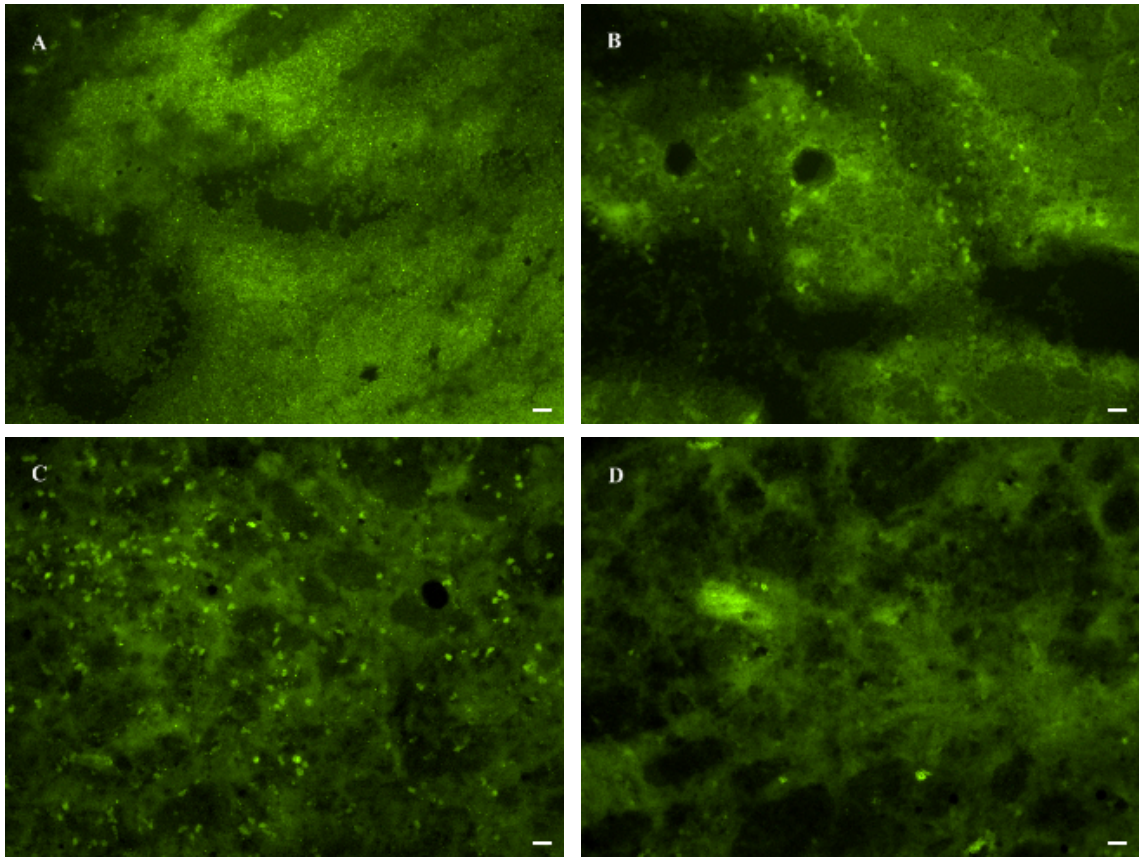


**Figure 5. Monocyte Infiltration Time Course.** All of the images were captured from a core region of a hemorrhage at 200x, and the scale bar is 20 $\mu$ m. (A) The 6h time point shows very few infiltrating GFP positive cells. (B) At the 24h time point GFP positive cell infiltration has begun, but has not yet peaked. (C) The 48h time point was the peak of GFP positive cell infiltration in our time course study. (D) At 7 days the number of GFP positive cells in brain parenchymal tissue has declined.

In both the core and peripheral counts we found an increase in the average number of cells per field during the first 48 hours, but by the 7-day time point the average number of GFP positive cells had begun to decrease. We found a significant increase in GFP positive cells in the core region at the 48-hour time point when compared to the 6-hour and 24-hour time points ( $p < 0.001$ ), but not when compared to the 7-day time point. Similarly, we found a significant increase in GFP positive cells in the peripheral region at

the 48 hours compared to the 6-hour time point ( $p < 0.001$ ), but the difference was not significant compared to the 24-hour and 7-day time points. Figure 6 summarizes these findings.



**Figure 6. GFP Positive Cells Counts of Inflammation Time Course.** The asterisks designate significant differences between treatment groups. Comparing the groups with a single asterisk to the 48-hour column represents a p value of  $< 0.001$ . Comparing the double asterisks to the 48-hour column represents a p value of  $< 0.01$ .

### ***Knockdown of GFP Positive Cell Infiltration***

Administration of the dimerizing agent, AP20187, successfully knocked down monocytes. Peripheral blood samples were taken from mice after the 4-day treatment protocol and analyzed by flow cytometry. The samples were prepared as mentioned above, but further analysis was required to interpret the data generated by the flow cytometer. Each sample was gated to include only events that were Red Dot positive, and within a size range determined by a side-scatter value between 100,000 and 700,000. This gating strategy aimed to include only nucleated (Red Dot positive) events roughly the size of a single cell (size condition, via side-scatter restriction). Events that fit into these two criteria were considered total leukocytes. From this grouping we separated leukocytes that were GFP positive, and labeled them monocytes/dendritic cells. A representative plot of the total leukocyte group is shown in Figure 7. The vertical axis is side-scatter, and representative of the size of the event. The horizontal axis is GFP, and the red vertical line is the division between GFP positive and negative events.

From this graph we were able to find the percentage of monocytes of the total leukocyte population. In the example displayed below, the vehicle group monocytes make up 14.1% of the sample's total leukocytes, whereas the dimerizer treated group monocytes only make up 0.3% of that sample's total leukocytes. Comparing 5 vehicle treated animals with 5 dimerizer treated animals, our dimerizer protocol knocked down monocytes in peripheral blood by 97.8% ( $p < 0.0005$ ).

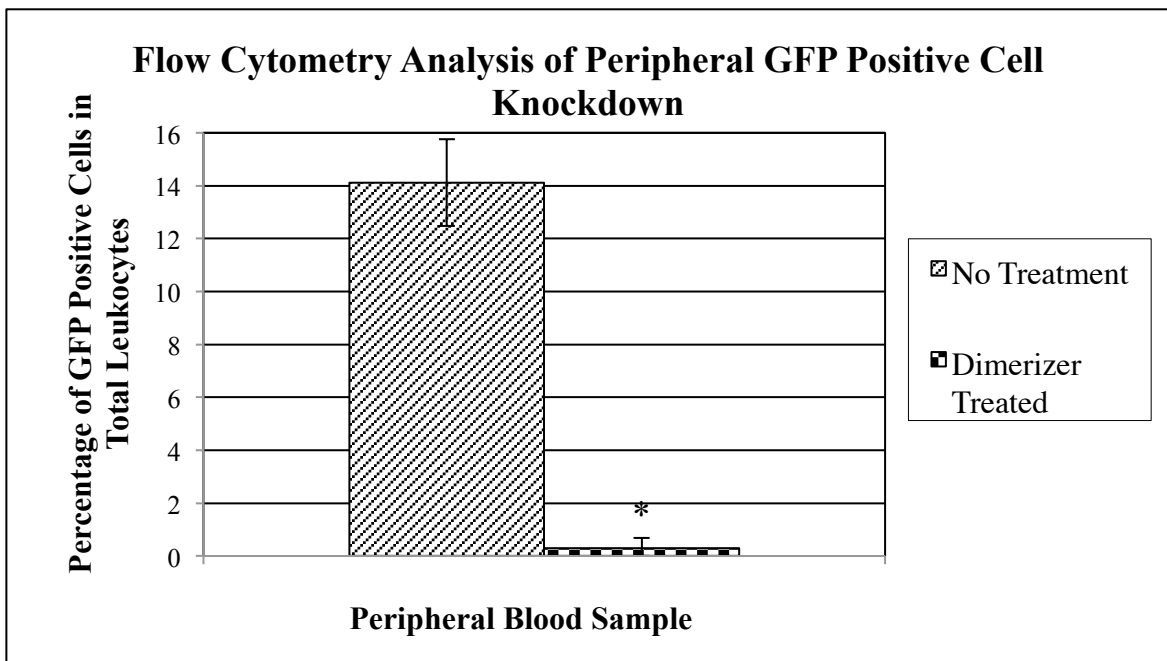
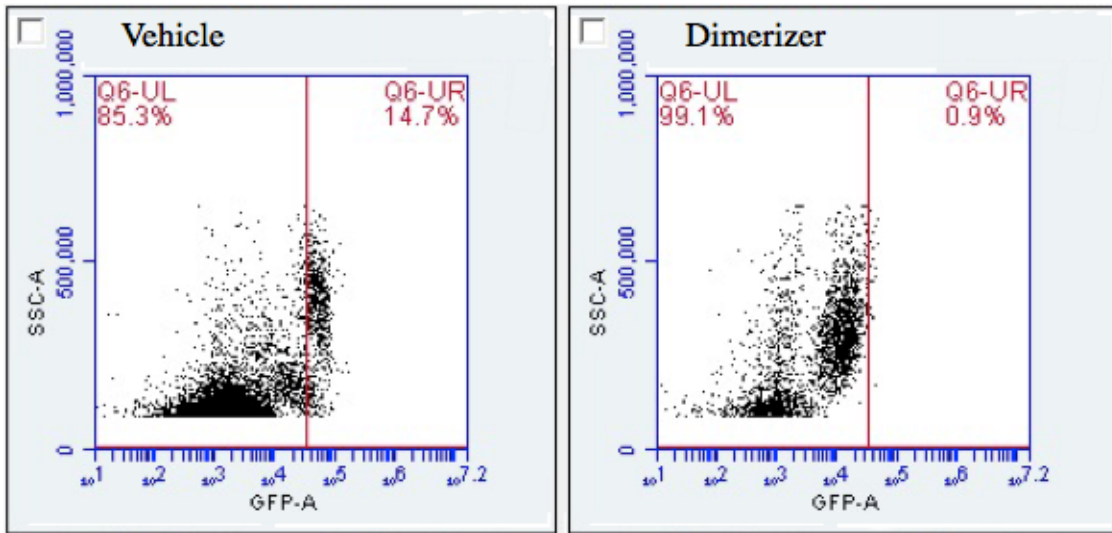


**Figure 7. Peripheral Blood Flow Cytometry Analysis.** A 95% confidence interval established that the knockdown was between 85-100%.

Brain tissue was harvested to investigate if the monocytes knock down was also present in brain parenchymal tissue following hemorrhage. Core and peripheral counts of

tissue from 6 dimerizer treated MAFIA mice sacrificed 48 hours post ICH were counted and compared to the group of 6 untreated MAFIA mice sacrificed at the 48 hour time point. We found a 68% reduction of infiltrating monocytes in the core, and a 64% reduction in the periphery (both p values < 0.01).

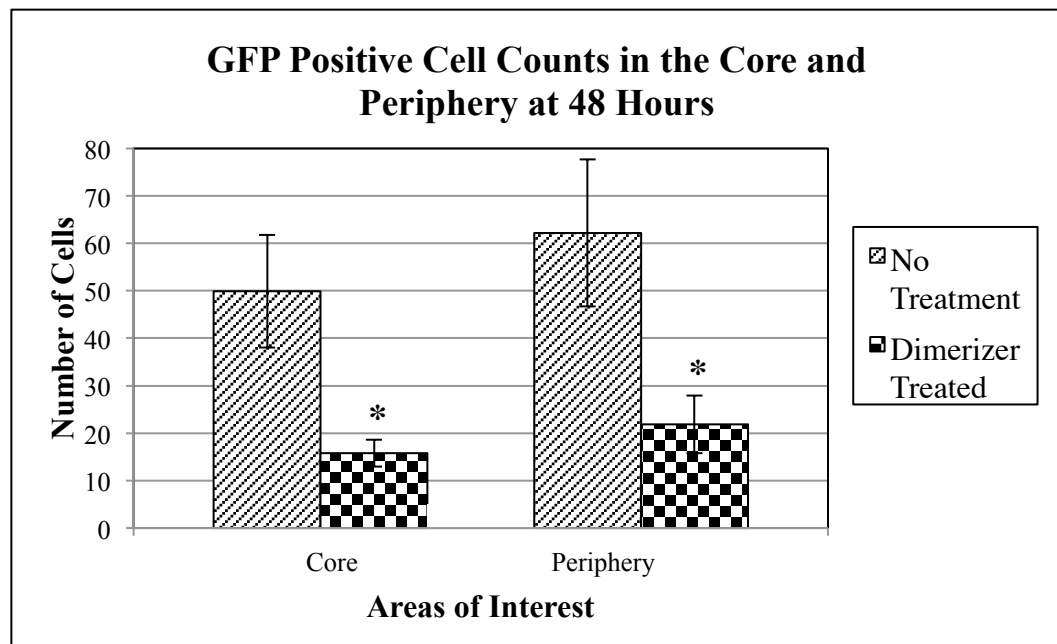


**Figure 8. Reduction of GFP Positive cells in brain tissue.** The dimerizer treated mice had significantly lower GFP positive cell in both the core and periphery of the lesion. Both groups contained six mice.

Consistent with other studies utilizing the MAFIA mouse model, our dimerizer treated mice lost weight<sup>55</sup>. The vehicle and dimerizer treated groups received the same amount of anesthesia, volume of fluid from injections, and hemorrhage surgery. However, the group receiving vehicle injections lost an average of 8.7% of their starting body weight by day 5, while the group receiving the dimerizer treatment lost an average of 20.0% of

their starting body weight by day 5 (Figure 9). The vehicle group also tended to gain back their weight by day 17 (beginning of MWM testing), whereas the dimerizer treated group still has an average weight loss of 19.6%. It should also be reported that 3 animals from the dimerizer treated group were found dead on days 14, 18, 19.

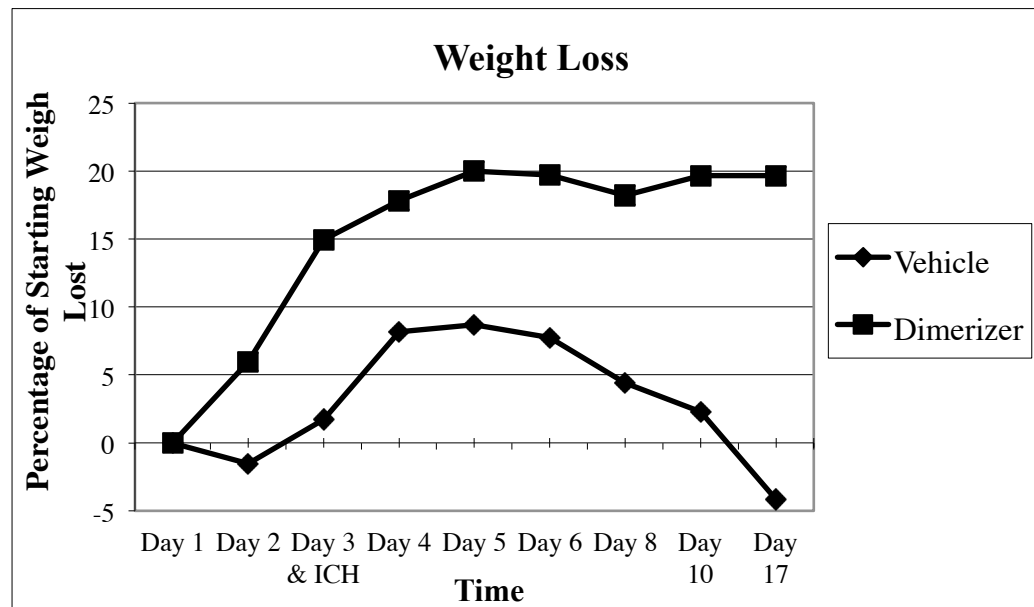


**Figure 9. Weight Loss Trend.** Both groups lost weight however, only vehicle group regained weight. Also it should be noted that the dimerizer treated group's weight lost started before injury.

### *Wire Grip Motor Test*

Wire grip testing was performed on days 4, 6, 8, and 10, and was scored as dictated by the grading rubric in Table 1. The vehicle treated group consisted of 7 mice, while the dimerizer treated group contained 6 mice. The 3 individual trail scores of each mouse were averaged and that average score was assigned as the mouse's score for that test. Then the scores of all the mice within a given group were averaged to obtain the group's performance for that day's trial. Figure 10 shows that both groups improved as

time progressed, however there was a significant difference between the two groups ( $p < 0.035$ ).

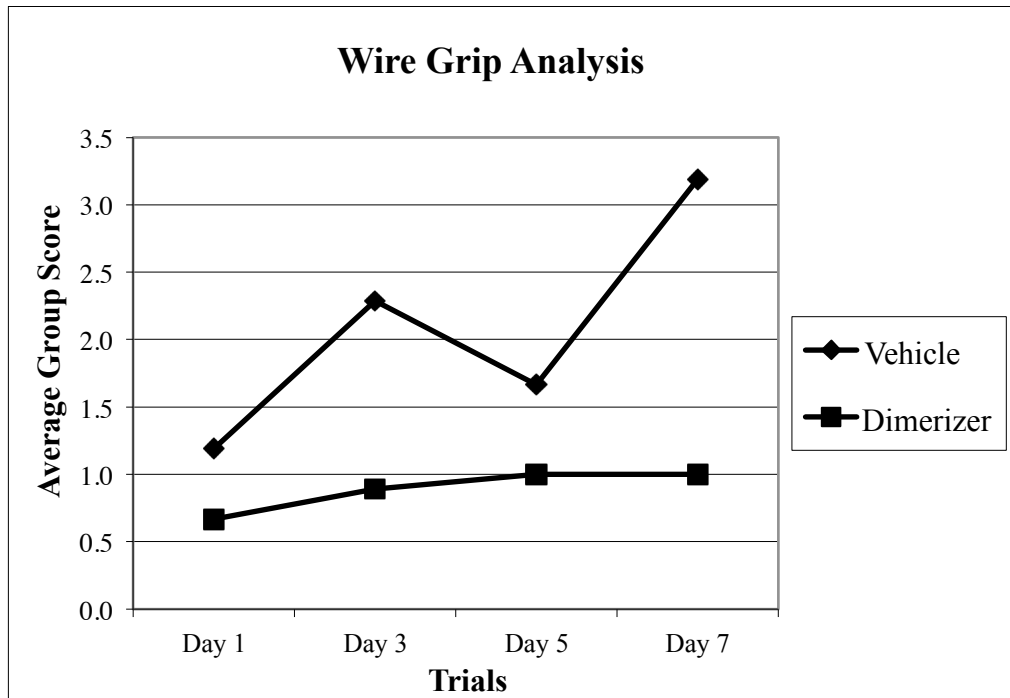


**Figure 10. Wire Grip Data.** In all four days of testing the vehicle group's average was higher than the dimerizer treated group. Also, the improvement shown by the vehicle group was greater than the improvement seen in the dimerizer group.

### *Morris Water Maze Test*

Morris water maze testing began 2 weeks following ICH and lasted for 3 days. The vehicle group consisted of 7 animals throughout all of the MWM trials. The dimerizer group began with 5 animals, but only 3 animals lived through the testing period. A significant difference was found between the vehicle and the dimerizer groups in hidden trials 3, 4, and 5 ( $p < 0.03$ ,  $0.003$ , and  $0.005$  respectively), however no significant difference was found between groups during the visible platform testing. The MWM data is summarized in Figure 11.

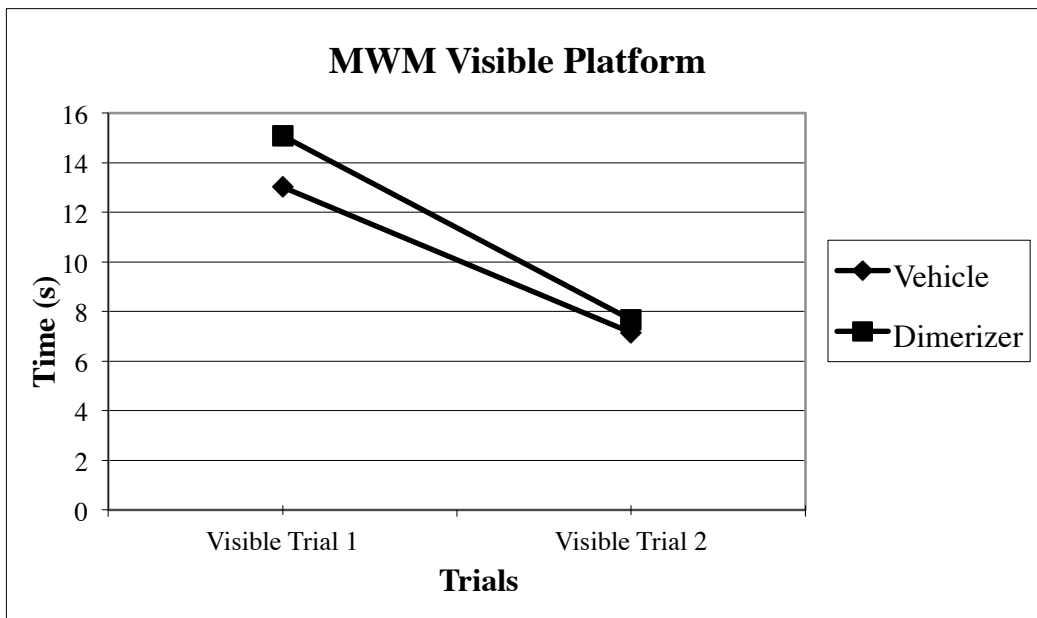
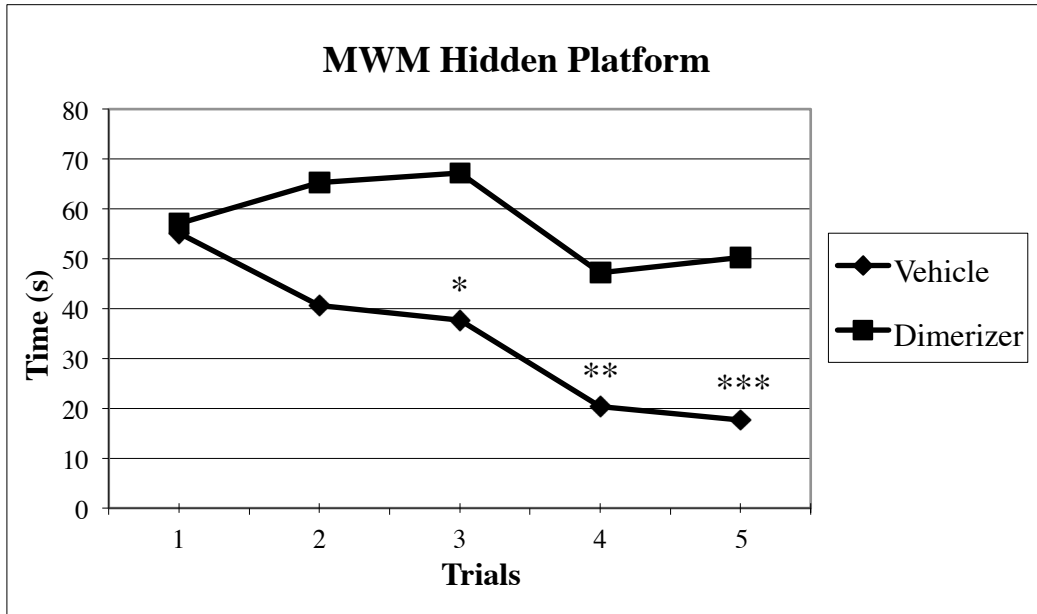


**Figure 11. Morris Water Maze Data.** The asterisks designate significant differences between treatment groups. The single, double, and triple asterisks correspond to difference between treatment group with p values of < 0.03, 0.003, 0.005, respectively. The dimerizer contained 6 mice and the vehicle group contained 7 mice.

### *Anatomical Abnormalities*

At the end of the study, on day 21, all mice were euthanatized and examined for evidence of an appropriately sized hemorrhage. Upon examination, the dimerizer group was found to have profound splenomegaly in comparison to the vehicle group (Figure 12). While it is believed that this is a complication of the transient monocyte depletion by the administration of AP20187, further study into the cause is recommended.

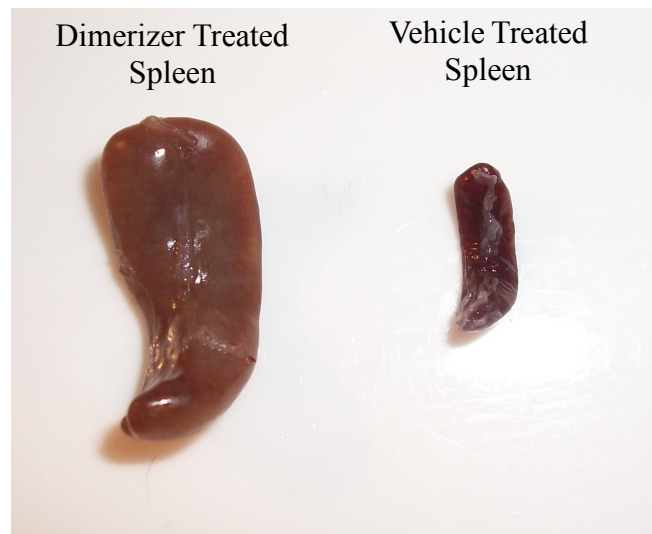


**Figure 12. Spleen Comparison.** Profound splenomegaly was observed in the dimerizer treated group after the mice were euthanized on day 21.

## DISCUSSION

### *Investigation of Immune Cell Infiltration*

Following intracerebral hemorrhage, the presence of immune cells in brain parenchymal tissue has been observed, but their role remains poorly understood. The large numbers of GFP cells observed in brain parenchymal tissue in this study suggest that monocytes are an important subset among the infiltrating leukocytes. Modulations of monocytes, and their function, are avenues for therapeutic development for patients suffering from ICH. Noting the lack of literature on monocyte involvement in ICH, this study offers a time line specifically for monocyte infiltration, explores the ability, and caveats, of the MAFIA mouse model to deplete monocytes, and finally investigates the functional outcome of mice that have been depleted of monocytes prior to undergoing ICH.

### *MAFIA Mice and Collagenase Induced ICH*

**MAFIA Mice:** The genetic alteration of MAFIA allowed for an elegant set of experiments in which we could visualize monocytes via their GFP tag, and also could selectively deplete them systemically by treatment with AP20187, a dimerizing agent. After treatment monocytes underwent a Fas-induced apoptosis, which importantly did not instigate an inflammatory response itself. It is also important to note that AP20187 was non-toxic when administered to wild type mice<sup>55</sup>. The MAFIA mouse model allowed us to visualize monocytes at any time point and the ability to deplete systemic monocytes for a

controlled amount of time, all without adding any confounding factors such as an inflammatory response.

A difficulty with the MAFIA mouse model in our study was interpreting the GFP positive cells. As seen in flow cytometric (Figure 7) and brain tissue (Figure 5) data, even with meticulous effort in sample preparation there still is notable background signal. In the flow cytometry data, there was not a well-defined distinction between GFP positive and GFP negative cells, instead there appeared to be a gradient of GFP labeling intensity. Also the large GFP positive cells with processes, which appeared only at the 7-day time point, indicate that monocytes either undergo morphological changes or some other cell type begins expressing GFP by the 7-day time point following ICH.

During GFP positive cell counts of brain parenchymal tissue to characterize the time course of monocytes infiltration the GFP positive cell ranged from 5-10 microns in diameter and appeared round without processes. At the 7-day time point we noticed GFP positive cells that were larger (10-15 microns) and also had processes. Figure 13 shows an example of the varied morphologies of GFP positive cells. Using multiple staining modalities would help clarify the end of the infiltration schedule, as well as illustrate morphological changes in monocytes. Determining the identity and fate of these large and processed cells is an important area for future study, as it will facilitate the interpretation of results from studies that use the MAFIA mouse model to study brain injury.

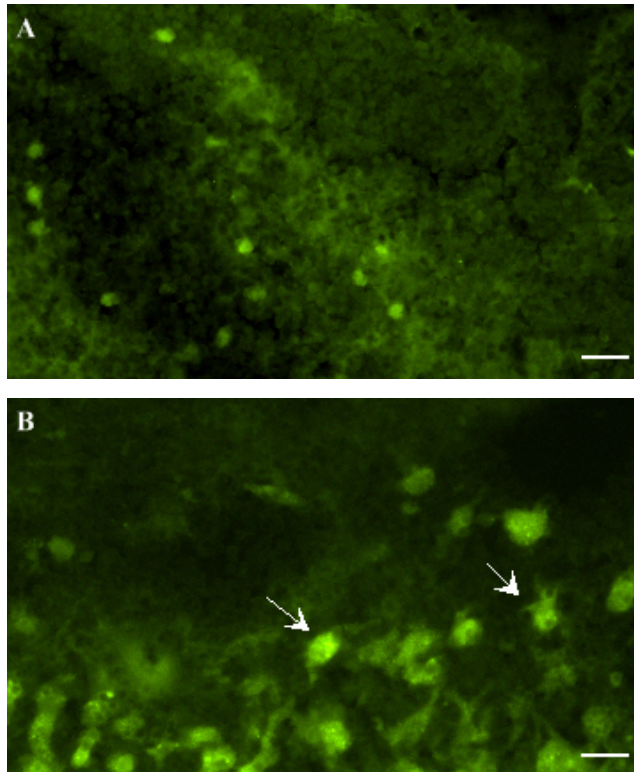


**Figure 13. Varied Morphologies of GFP Positive Cell in Brain Tissue.** The images were captured from a peripheral region of a hemorrhage at 200x, and the scale bar is 20µm. (A) This tissue was harvested at the 24-hour time point following hemorrhage, and illustrates the small, circular, GFP positive cells found in all time points. (B) This tissue was harvested at the 7-day time point, and shows both the small, circular GFP positive cells as well as the larger, processed cells highlighted by the arrows.

**Collagenase Induced ICH:** The two most commonly used intracerebral hemorrhage models for studies with mice are an autologous blood injection, and the injection of collagenase. We elected to use the collagenase induced hemorrhage model because it causes active bleeding within brain tissue, via disruption of the basement membrane of capillaries and small vessels. Our study investigated leukocyte infiltration, and thus the physical disruption in the vasculature was deemed an important pathological characteristic of ICH to be replicated in our injury model.

However, our injury model does have limitations and disadvantages. Bacteria-derived collagenase is known to have toxic effects on brain parenchymal cells<sup>5</sup>, and the hemorrhage has notable variability in hematoma size between animals from the diffusion and/or activity of the enzyme. As with all studies of brain injury with rodents, the substantially lower ratio of white to gray matter in the mouse brain limits their relevance when compared to the human ailment. Even with acknowledging these limitations, our study still is able to add to the field's understanding of the roles monocytes play following ICH.

#### ***Administration of AP20187 and Knockdown of Monocytes***

The treatment protocol of AP20187, the dimerizing agent, produced significant knockdown in our model (data shown in Figures 7 and 8). A number of pilot studies were conducted (data not shown) and we found that when the first dose was given intravenously a more thorough knockdown was observed. Based on the substantial knockdown seen in peripheral blood while using a total of 40 $\mu$ L per animal over the course of 4 days, and taking into account the considerable cost of AP20187, we felt the treatment protocol described above best suited our study design.

We noticed a substantial weight loss side effect in the dimerizer treated group, which was consistent with previously published studies<sup>55</sup>. Ultimately, we were unable to adequately control for this weight loss, and it remained as a potential confounding factor in our study. Within 24 hours of the first dimerizer treatment the mice began to lose weight, and they remained underweight the entire length of the study, even though

dimerizer was only administered during the first 4 days. Identifying the cause of the weight loss, and a proper control group would benefit future studies.

### ***Functional Outcome of Monocyte Depleted Mice Undergoing ICH***

In both the wire grip and Morris Water Maze testing the dimerizer-treated mice performed significantly worse than the vehicle group. The wire grip test measure motor function acutely after ICH, and is used to examine hemiplegia. The Morris Water Maze test measures a combination of both motor function and cognitive processing demonstrated by swimming ability and spatial learning and memory.

The monocyte-depleted group also had a mortality rate of 50% by the end of the study, whereas no mortality was observed in the vehicle treated group (Figure 14). Together these findings indicate that undergoing intracerebral hemorrhage while depleted of monocytes worsens both mortality and functional outcomes. Further research is required to determine if the deficit in the monocyte-depleted group is transient or chronic.

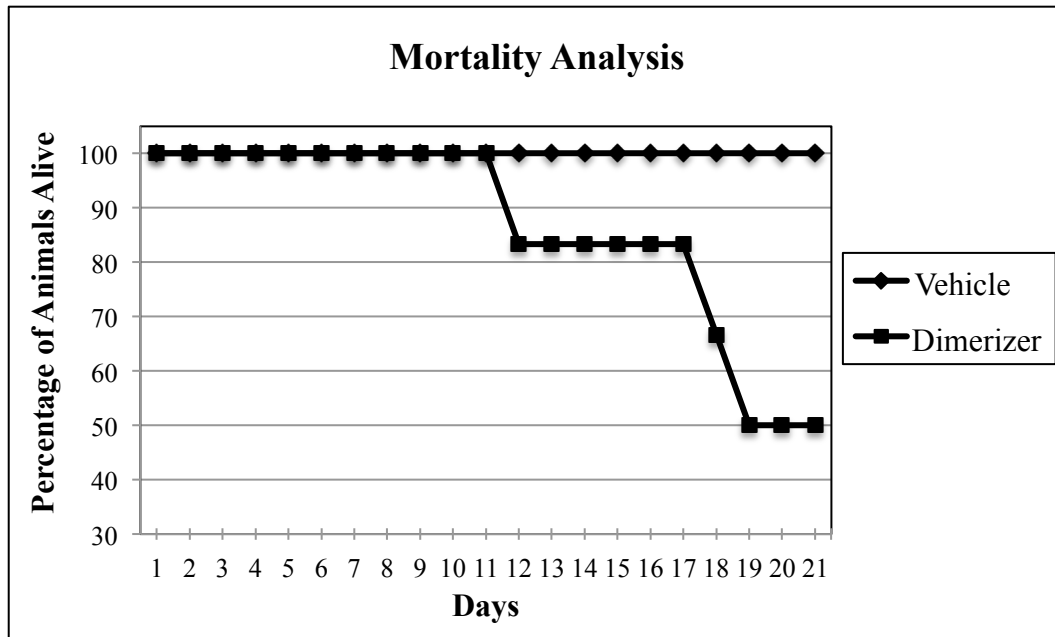


**Figure 14. Mortality Analysis.** Over the 3-week study 50% mortality was observed in the monocyte-depleted group, while no mortality was seen in the vehicle group.

### *Avenues for Future Study*

As preliminary study into the presence and role of monocytes in brain parenchymal tissue following an intracerebral hemorrhage, a number of future study objectives were identified. Further investigation into the specificity of GFP expression, and the causes of the splenomegaly and weight loss in the dimerizer treated group will strengthen the findings here and the continued use of the MAFIA mouse model. A proper control for weight loss, and a wider variety of motor and cognitive testing will confirm and further characterize the deficits identified in the current study.

In summary, using the macrophage Fas-induced apoptosis mouse model, this study documents a time course of monocyte infiltration into brain parenchymal tissue following

hemorrhage. Future studies strengthening the MAFIA mouse model and clarifying our findings will potentially open the door for therapeutic modulation of monocyte function.

## LIST OF JOURNAL ABBREVIATIONS

|                             |   |
|-----------------------------|---|
| J. Cereb. Blood Flow Metab. | Journal of Cerebral Blood Flow & Metabolism |
| J. Leukoc. Biol.            | Journal of Leukocyte Biology                |
| J. Med. Neurosurg           | Journal Medical Neurosurgery                |
| J. Neurochem.               | Journal of Neurochemistry                   |
| J. Neurosci.                | Journal of Neuroscience                     |
| Lancet Neurol               | Lancet Neurology                            |
| N. Engl. J. Med             | New England Journal of Medicine             |
| Neurosurg. Focus            | Neurosurgical Focus                         |
| Semin Neurol.               | Semin Neurology                             |

## REFERENCES

1. Lloyd-Jones D, Adams R, Carnethon M, et al. Heart disease and stroke statistics--2009 update: a report from the American Heart Association Statistics Committee and Stroke Statistics Subcommittee. *Circulation*. 2009;119(3):480–486. doi:10.1161/CIRCULATIONAHA.108.191259.
2. Center for Disease Control. CDC - DHDSP - Types of Stroke. Available at: [http://www.cdc.gov/stroke/types\\_of\\_stroke.htm](http://www.cdc.gov/stroke/types_of_stroke.htm). Accessed January 3, 2013.
3. Qureshi AI, Mendelow AD, Hanley DF. Intracerebral haemorrhage. *Lancet*. 2009;373(9675):1632–1644. doi:10.1016/S0140-6736(09)60371-8.
4. Dihanich M, Kaser M, Reinhard E, Cunningham D, Monard D. Prothrombin mRNA is expressed by cells of the nervous system. *Neuron*. 1991;6(4):575–581. doi:10.1016/0896-6273(91)90060-D.
5. Xi G, Keep RF, Hoff JT. Mechanisms of brain injury after intracerebral haemorrhage. *Lancet Neurol*. 2006;5(1):53–63. doi:10.1016/S1474-4422(05)70283-0.
6. Qureshi AI, Tuhim S, Broderick JP, Batjer HH, Hondo H, Hanley DF. Spontaneous intracerebral hemorrhage. *N. Engl. J. Med.* 2001;344(19):1450–1460. doi:10.1056/NEJM200105103441907.
7. Dennis MS, Burn JP, Sandercock PA, Bamford JM, Wade DT, Warlow CP. Long-term survival after first-ever stroke: the Oxfordshire Community Stroke Project. *Stroke*. 1993;24(6):796–800.
8. Schmidt EV, Smirnov VE, Ryabova VS. Results of the seven-year prospective study of stroke patients. *Stroke*. 1988;19(8):942–949.
9. Kojima S, Omura T, Wakamatsu W, et al. Prognosis and disability of stroke patients after 5 years in Akita, Japan. *Stroke*. 1990;21(1):72–77.
10. Daverat P, Castel JP, Dartigues JF, Orgogozo JM. Death and functional outcome after spontaneous intracerebral hemorrhage. A prospective study of 166 cases using multivariate analysis. *Stroke*. 1991;22(1):1–6.
11. Gong Y, Hua Y, Keep RF, Hoff JT, Xi G. Intracerebral hemorrhage: effects of aging on brain edema and neurological deficits. *Stroke*. 2004;35(11):2571–2575. doi:10.1161/01.STR.0000145485.67827.d0.
12. Gong C, Hoff JT, Keep RF. Acute inflammatory reaction following experimental intracerebral hemorrhage in rat. *Brain Research*. 2000;871(1):57–65. doi:10.1016/S0006-8993(00)02427-6.
13. Babu R, Bagley JH, Di C, Friedman AH, Adamson C. Thrombin and hemin as central factors in the mechanisms of intracerebral hemorrhage-induced secondary brain injury and as potential targets for intervention. *Neurosurg Focus*. 2012;32(4):E8. doi:10.3171/2012.1.FOCUS11366.
14. Fujii Y, Takeuchi S, Sasaki O, Minakawa T, Tanaka R. Multivariate analysis of predictors of hematoma enlargement in spontaneous intracerebral hemorrhage. *Stroke*. 1998;29(6):1160–1166.
15. Kazui S, Minematsu K, Yamamoto H, Sawada T, Yamaguchi T. Predisposing factors to enlargement of spontaneous intracerebral hematoma. *Stroke*. 1997;28(12):2370–2375.
16. Brott T, Broderick J, Kothari R, et al. Early hemorrhage growth in patients with intracerebral hemorrhage. *Stroke*. 1997;28(1):1–5.

17. Eljovich L, Patel PV, Hemphill JC 3rd. Intracerebral hemorrhage. *Semin Neurol.* 2008;28(5):657–667. doi:10.1055/s-0028-1105974.
18. Xi G, Reiser G, Keep RF. The role of thrombin and thrombin receptors in ischemic, hemorrhagic and traumatic brain injury: deleterious or protective? *J. Neurochem.* 2003;84(1):3–9.
19. Lee KR, Drury I, Vitarbo E, Hoff JT. Seizures induced by intracerebral injection of thrombin: a model of intracerebral hemorrhage. *J. Neurosurg.* 1997;87(1):73–78.
20. Xi G, Wagner KR, Keep RF, et al. Role of blood clot formation on early edema development after experimental intracerebral hemorrhage. *Stroke.* 1998;29(12):2580–2586.
21. Xi G, Keep RF, Hua Y, Xiang J, Hoff JT. Attenuation of Thrombin-Induced Brain Edema by Cerebral Thrombin Preconditioning. *Stroke.* 1999;30(6):1247–1255. doi:10.1161/01.STR.30.6.1247.
22. Striggow F, Riek M, Breder J, Henrich-Noack P, Reymann KG, Reiser G. The protease thrombin is an endogenous mediator of hippocampal neuroprotection against ischemia at low concentrations but causes degeneration at high concentrations. *Proceedings of the National Academy of Sciences.* 2000;97(5):2264–2269. doi:10.1073/pnas.040552897.
23. Suzuki M, Ogawa A, Sakurai Y, et al. Thrombin activity in cerebrospinal fluid after subarachnoid hemorrhage. *Stroke.* 1992;23(8):1181–1182. doi:10.1161/01.STR.23.8.1181.
24. Ducruet AF, Zacharia BE, Hickman ZL, et al. The complement cascade as a therapeutic target in intracerebral hemorrhage. *Experimental Neurology.* 2009;219(2):398–403. doi:10.1016/j.expneurol.2009.07.018.
25. Hua Y, Xi G, Keep RF, Hoff JT. Complement activation in the brain after experimental intracerebral hemorrhage. *J. Neurosurg.* 2000;92(6):1016–1022. doi:10.3171/jns.2000.92.6.1016.
26. Coughlin SR. Thrombin signaling and protease-activated receptors. *Nature.* 2000;407(6801):258–264. doi:10.1038/35025229.
27. Donovan FM, Pike CJ, Cotman CW, Cunningham DD. Thrombin Induces Apoptosis in Cultured Neurons and Astrocytes via a Pathway Requiring Tyrosine Kinase and RhoA Activities. *J. Neurosci.* 1997;17(14):5316–5326.
28. Grand R, Turnell A, Grabham P. Cellular Consequences of Thrombin-Receptor Activation. *The Biochemical Journal.* 1996;313:353–368.
29. Ohnishi M, Katsuki H, Fujimoto S, Takagi M, Kume T, Akaike A. Involvement of thrombin and mitogen-activated protein kinase pathways in hemorrhagic brain injury. *Experimental Neurology.* 2007;206(1):43–52. doi:10.1016/j.expneurol.2007.03.030.
30. Wu J, Yang S, Xi G, et al. Microglial Activation and Brain Injury after Intracerebral Hemorrhage. *Acta neurochirurgica. Supplement.* 2008;105:59–65.
31. Epstein FH, Barnes PJ, Karin M. Nuclear Factor- $\kappa$ B — A Pivotal Transcription Factor in Chronic Inflammatory Diseases. *New England Journal of Medicine.* 1997;336(15):1066–1071. doi:10.1056/NEJM199704103361506.

32. Hickenbottom SL, Grotta JC, Strong R, Denner LA, Aronowski J. Nuclear Factor- $\kappa$ B and Cell Death After Experimental Intracerebral Hemorrhage in Rats. *Stroke*. 1999;30(11):2472–2478. doi:10.1161/01.STR.30.11.2472.
33. Zazulia AR, Diring MN, Derdeyn CP, Powers WJ. Progression of Mass Effect After Intracerebral Hemorrhage. *Stroke*. 1999;30(6):1167–1173. doi:10.1161/01.STR.30.6.1167.
34. Wang J, Doré S. Inflammation after intracerebral hemorrhage. *J Cereb Blood Flow Metab*. 2007;27(5):894–908. doi:10.1038/sj.jcbfm.9600403.
35. Hwang BY, Appelboom G, Ayer A, et al. Advances in Neuroprotective Strategies: Potential Therapies for Intracerebral Hemorrhage. *Cerebrovascular Diseases*. 2011;31(3):211–222. doi:10.1159/000321870.
36. Wang J, Tsirka S. Contribution of extracellular proteolysis and microglia to intracerebral hemorrhage. *Neurocritical Care*. 2005;3(1):77–85.
37. Hanisch U. Microglia as a source and target of cytokines. *Glia*. 2002;40(2):140–155.
38. Wang J, Tsirka SE. Tuftsin Fragment 1–3 Is Beneficial When Delivered After the Induction of Intracerebral Hemorrhage. *Stroke*. 2005;36(3):613–618. doi:10.1161/01.STR.0000155729.12931.8f.
39. Emsley HCA, Tyrrell PJ. Inflammation and Infection in Clinical Stroke. *J Cereb Blood Flow Metab*. 2002;22(12):1399–1419. doi:10.1097/01.WCB.0000037880.62590.28.
40. Zhu X, Tao L, Tejima-Mandeville E, et al. Plasmalemma permeability and necrotic cell death phenotypes after intracerebral hemorrhage in mice. *Stroke*. 2012;43(2):524–531. doi:10.1161/STROKEAHA.111.635672.
41. Wang J, Tsirka SE. Neuroprotection by inhibition of matrix metalloproteinases in a mouse model of intracerebral haemorrhage. *Brain*. 2005;128(7):1622–1633. doi:10.1093/brain/awh489.
42. Xi G, Keep RF, Hoff JT. Erythrocytes and delayed brain edema formation following intracerebral hemorrhage in rats. *Journal of neurosurgery*. 1998;89:991–996.
43. Yang G-Y, Betz AL, Chenevert TL, Brunberg JA, Hoff JT. Experimental intracerebral hemorrhage: relationship between brain edema, blood flow, and blood-brain barrier permeability in rats. *Journal of neurosurgery*. 1994;81:93–102.
44. Leira R, Davalos A, Silva Y, et al. Early neurologic deterioration in intracerebral hemorrhage: Predictors and associated factors. *Neurology*. 2004;63(3):461–467. doi:10.1212/01.WNL.0000133204.81153.AC.
45. Weiss SJ. Tissue Destruction by Neutrophils. *New England Journal of Medicine*. 1989;320(6):365–376. doi:10.1056/NEJM198902093200606.
46. Szmydynger-Chodobska J, Strazielle N, Gandy JR, et al. Posttraumatic invasion of monocytes across the blood–cerebrospinal fluid barrier. *Journal of Cerebral Blood Flow & Metabolism*. 2011;32(1):93–104. doi:10.1038/jcbfm.2011.111.
47. Chen Y, Hallenbeck JM, Ruetzler C, et al. Overexpression of Monocyte Chemoattractant Protein 1 in the Brain Exacerbates Ischemic Brain Injury and Is Associated With Recruitment of Inflammatory Cells. *Journal of Cerebral Blood Flow & Metabolism*. 2003:748–755. doi:10.1097/01.WCB.0000071885.63724.20.

48. Rollins BJ. Chemokines. *Blood*. 1997;90(3):909–928.
49. Minino, M.P.H. A, Murphy, B.S. S, Xu, M.D. J, Kochanek, M.A. K, Division of Vital Statistics. *National Vital Statistics Reports. Deaths: Final Data for 2008*. Center for Disease Control; 2011:127.
50. Qureshi AI, Suri MFK, Nasar A, et al. Changes in Cost and Outcome Among US Patients With Stroke Hospitalized in 1990 to 1991 and Those Hospitalized in 2000 to 2001. *Stroke*. 2007;38(7):2180–2184. doi:10.1161/STROKEAHA.106.467506.
51. Feigin VL, Lawes CM, Bennett DA, Anderson CS. Stroke epidemiology: a review of population-based studies of incidence, prevalence, and case-fatality in the late 20th century. *The Lancet Neurology*. 2003;2(1):43–53. doi:10.1016/S1474-4422(03)00266-7.
52. Steiner T, Vincent C, Morris S, Davis S, Vallejo-Torres L, Christensen MC. Neurosurgical Outcomes After Intracerebral Hemorrhage: Results of the Factor Seven for Acute Hemorrhagic Stroke Trial (FAST). *Journal of Stroke and Cerebrovascular Diseases*. 2011;20(4):287–294. doi:10.1016/j.jstrokecerebrovasdis.2009.12.008.
53. Mayer SA, Brun NC, Begtrup K, et al. Recombinant Activated Factor VII for Acute Intracerebral Hemorrhage. *New England Journal of Medicine*. 2005;352(8):777–785. doi:10.1056/NEJMoa042991.
54. Elliott J, Smith M. The Acute Management of Intracerebral Hemorrhage. *Anesthesia & Analgesia*. 2010;110(5):1419–1427. doi:10.1213/ANE.0b013e3181d568c8.
55. Burnett SH, Kershen EJ, Zhang J, et al. Conditional macrophage ablation in transgenic mice expressing a Fas-based suicide gene. *J. Leukoc. Biol*. 2004;75(4):612–623. doi:10.1189/jlb.0903442.

VITA

[REDACTED]

[REDACTED] [REDACTED]  
[REDACTED]  
[REDACTED]  
[REDACTED]

[REDACTED] [REDACTED]

[REDACTED] [REDACTED]

[REDACTED] [REDACTED]  
[REDACTED]

[REDACTED] [REDACTED]  
[REDACTED]  
[REDACTED]  
[REDACTED]  
[REDACTED]  
[REDACTED]

[REDACTED] [REDACTED]  
[REDACTED] [REDACTED]  
[REDACTED]  
[REDACTED]  
[REDACTED]  
[REDACTED]  
[REDACTED]  
[REDACTED]

[REDACTED] [REDACTED]  
[REDACTED]  
[REDACTED]  
[REDACTED]  
[REDACTED]  
[REDACTED]  
[REDACTED]  
[REDACTED]

[REDACTED] [REDACTED]  
[REDACTED]

[REDACTED] [REDACTED]

[REDACTED]

[REDACTED]  
[REDACTED]  
[REDACTED]  
[REDACTED]

[REDACTED] [REDACTED]  
[REDACTED]  
[REDACTED]  
[REDACTED]  
[REDACTED]  
[REDACTED]  
[REDACTED]

[REDACTED] [REDACTED]  
[REDACTED]  
[REDACTED]  
[REDACTED]  
[REDACTED]

[REDACTED]

[REDACTED] [REDACTED]  
[REDACTED]  
[REDACTED]

[REDACTED] [REDACTED]  
[REDACTED]  
[REDACTED]  
[REDACTED]  
[REDACTED]  
[REDACTED]